

# Locating and Editing Factual Associations in Mamba

Arnab Sen Sharma\*, David Atkinson, and David Bau

Khoury College of Computer Sciences, Northeastern University

## Abstract

We investigate the mechanisms of factual recall in the Mamba state space model. Our work is inspired by previous findings in autoregressive transformer language models suggesting that their knowledge recall is localized to particular modules at specific token locations; we therefore ask whether factual recall in Mamba can be similarly localized. To investigate this, we conduct four lines of experiments on Mamba. First, we apply causal tracing or interchange interventions to localize key components inside Mamba that are responsible for recalling facts, revealing that specific components within middle layers show strong causal effects at the last token of the subject, while the causal effect of intervening on later layers is most pronounced at the last token of the prompt, matching previous findings on autoregressive transformers. Second, we show that rank-one model editing methods can successfully insert facts at specific locations, again resembling findings on transformer models. Third, we examine the linearity of Mamba’s representations of factual relations. Finally we adapt attention-knockout techniques to Mamba to dissect information flow during factual recall. We compare Mamba directly to a similar-sized transformer and conclude that despite significant differences in architectural approach, when it comes to factual recall, the two architectures share many similarities.

## 1 Introduction

Studies of autoregressive transformer language models’ (LMs) processing of factual statements such as *The Eiffel Tower is located in Paris*, have identified a localized pattern of internal computations when recalling facts (Meng et al., 2022a;b; Geva et al., 2023; Hernandez et al., 2023; Nanda et al., 2023), and have further found that those LMs can be edited by making single-layer rank-one changes in model parameters to alter a specific fact. Although these localized phenomena appear to generalize across transformer LMs, the extent to which similar locality might appear in very different architectures—such as recurrent networks (RNNs)—has not yet been investigated.

In this paper we investigate the internal mechanisms of Mamba (Gu & Dao, 2023), a recently-proposed state-space language model, a type of RNN that achieves per-parameter performance that is competitive with transformers. Specifically, we ask whether factual recall within Mamba exhibits locality similar to the patterns observed in autoregressive transformer language models.

Our paper is a case study confronting a key methodological challenge that broadly faces interpretability researchers: as state-of-the-art neural network architectures evolve, we must ask, can the detailed analytical methods and tools developed for one neural architecture, such as transformer LMs, be generalized and applied to a different neural architecture such as Mamba? In this we are able to answer the question with a qualified “yes”: we find that many of the methods used to analyze transformers can also provide insights on Mamba. We also discuss mismatches—that is, interpretation methods (such as path-dependent attention patching) that do not transfer to Mamba as easily due to architectural differences.

We begin by studying whether activation patching (Wang et al., 2022) can be successfully applied to Mamba. Known variously as causal mediation analysis (Vig et al., 2020), causal tracing (Meng et al., 2022a), and interchange interventions (Geiger et al., 2021), activation patching techniques can successfully identify specific model components in transformer LMs that play crucial roles in performing a task. We ask whether Mamba can be productively studied the same way, even though

\*Correspondence to [sensharma.a@northeastern.edu](mailto:sensharma.a@northeastern.edu), Code available at [github.com/arnab-api/romba](https://github.com/arnab-api/romba)

the architectural components of Mamba are very different: for example, instead of attention heads and MLP modules, Mamba is composed of convolutions, gates, and state-space modules. To answer, we adapt activation patching to Mamba, and ask if any sparsity patterns emerge which provide insights into the respective roles of its components.

We also study whether rank-one model editing can be applied to Mamba. While studies of transformers (Meng et al., 2022a;b; Hase et al., 2024) have found that there are a range of MLP modules within which factual knowledge can be inserted by making a single rank-one change in parameters, Mamba does not have MLP modules, so we ask if there are any other modules that can be similarly edited to insert knowledge. As with previous studies of transformers, the key question is whether factual associations can be edited with both specificity (without interfering with unrelated facts) and generalization (while remaining robust to rewordings of the edited fact).

Finally, we apply methods for understanding the overall information flows in Mamba. Inspired by the linearity findings of Hernandez et al. (2023), we measure the linearity of the relations between subject and object embeddings. And inspired by Geva et al. (2023), we examine information flow by adapting attention-blocking methods to the attention-free Mamba architecture.

In this work we conduct our experiments on Mamba-2.8b, the largest available LM in Mamba family, and for comparison we conduct the same experiments on the similarly sized Pythia-2.8b (Biderman et al., 2023) autoregressive transformer LM.

## 2 Background on Mamba

Mamba, introduced in Gu & Dao (2023), is a recent family of language models based on state space models (SSMs). SSMs are designed to model the evolution of hidden state across time with a first-order differential equation (Koopman et al., 1999; Durbin & Koopman, 2012), and when they are used as the recurrent state of an RNN, they can enable highly efficient parallelized training (Gu et al., 2021). To achieve good performance in language modeling, the Mamba SSM introduces input-dependent parameterization or *selective*-SSM instead of the traditional time-invariant SSMs. Mamba uses a special architecture called **MambaBlock**<sup>1</sup>, which is stacked homogeneously, replacing both attention and MLP blocks used in transformer layers. Here, we focus on the different operations performed inside a MambaBlock.

Formally, Mamba is an autoregressive language model:  $M : \mathcal{X} \rightarrow \mathcal{Y}$  over a vocabulary  $\mathcal{V}$  that maps a sequence of tokens  $x = [x_1, x_2, \dots, x_T] \in \mathcal{X}$ ,  $x_i \in \mathcal{V}$  to  $y \in \mathcal{Y} \subset \mathbb{R}^{|\mathcal{V}|}$  which is a probability distribution over the next token continuations of  $x$ . Similar to other deep LMs, in Mamba, a token  $x_i$  is first embedded to a hidden state of size  $d$  as  $h_i^{(0)} = \text{emb}(x_i)$ . Then  $h_i^{(0)}$  is transformed sequentially by a series of MambaBlocks. The hidden state  $h_i^{(\ell)}$  after the  $\ell^{\text{th}}$  (1-indexed) MambaBlock is computed as follows:

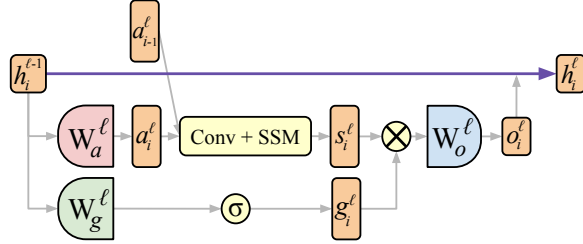


Figure 1: Architecture of a MambaBlock. Projection matrices  $W_a^\ell$  and  $W_g^\ell$  have the shape  $2d \times d$ , while  $W_o^\ell$  has the shape  $d \times 2d$ .  $h, a, g, s$ , and  $o$  are intermediate states of a token representation.  $\sigma$  is SiLU activation and  $\otimes$  is elementwise multiplication. *Conv + SSM* operation abstracts the Conv1D and *selective*-SSM operations.

$$h_i^{(\ell)} = h_i^{(\ell-1)} + o_i^{(\ell)} \quad (1)$$

where  $o_i^{(\ell)}$  is the output of  $\ell^{\text{th}}$  MambaBlock for the  $i^{\text{th}}$  token

$$o_i^{(\ell)} = \text{MambaBlock}^{(\ell)}(h_1^{(\ell-1)}, h_2^{(\ell-1)}, \dots, h_i^{(\ell-1)}) = W_o^{(\ell)}(s_i^{(\ell)} \otimes g_i^{(\ell)}) \quad (2)$$

Here,  $\otimes$  represents element-wise multiplication or Hadamard product.  $s_i^{(\ell)}$  is calculated as:

<sup>1</sup>In their paper, Gu & Dao (2023) call this component Mamba—the same name as the LM family.

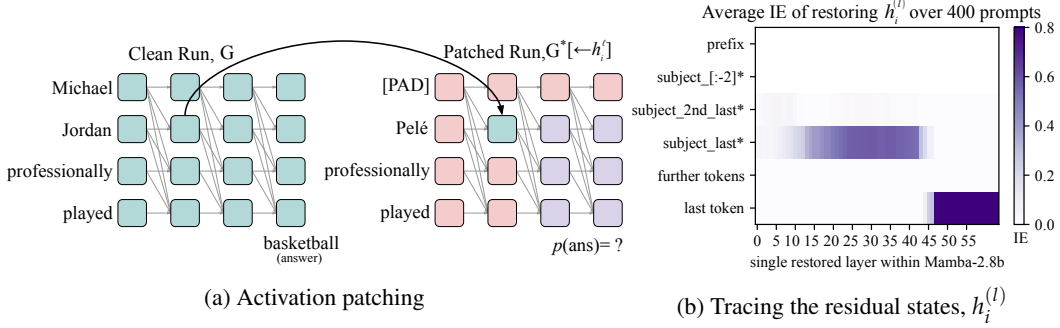


Figure 2: **(a)** Activation patching. A state from the clean run  $G$  is *patched* into its corresponding position in  $G^*$ . This has a downstream effect of potentially changing all the states that depend on the patched state in  $G^* [\leftarrow h_i^{(\ell)}]$ . **(b)** Average indirect effect of applying causal tracing on residual stream states ( $h_i^{(\ell)}$  in Figure 1) across 400 different facts.

$$a_i^{(\ell)} = W_a^{(\ell)} h_i^{(\ell)} \quad (3)$$

$$c_1^{(\ell)}, c_2^{(\ell)}, \dots, c_i^{(\ell)} = \text{SiLU}\left(\text{Conv1D}\left(a_1^{(\ell)}, a_2^{(\ell)}, \dots, a_i^{(\ell)}\right)\right) \quad (4)$$

$$s_i^{(\ell)} = \text{selective-SSM}\left(c_1^{(\ell)}, c_2^{(\ell)}, \dots, c_i^{(\ell)}\right) \quad (5)$$

We abstract the operations in Equations 4 and 5 as the **Conv + SSM** operation in Figure 1. At a high level, Conv + SSM brings information from the past token representations to the current token representation. The purpose is similar to the *attention* blocks in transformer LMs. But, unlike attention operation, Conv + SSM scales *linearly* with the context length and thereby enjoys faster inference speed and longer context limits. See Gu & Dao (2023) for details.

The output of the other path  $g_i^{(\ell)}$  (that does not pass through Conv + SSM operation) is a gating mechanism that regulates the information flow. This gating mechanism resemble parts of LSTM (Hochreiter & Schmidhuber, 1997) and GRU (Cho et al., 2014) networks, where similar gates control selective updates of recurrent state.

$$g_i^{(\ell)} = \text{SiLU}\left(W_g^{(\ell)} h_i^{(\ell-1)}\right) \quad (6)$$

In the remainder of the paper, we aim to characterize the role of the components of Mamba in factual recall by adapting tools that have previously been used to analyze transformers. In Section 3, we apply activation patching to localize factual recall as in Meng et al. (2022a), testing the roles of states  $s_i$ ,  $g_i$ , and  $o_i$  at all layers. In Section 4, following Meng et al. (2022a); Hase et al. (2024), we test rank-one edits of facts across components  $W_a$ ,  $W_g$ , and  $W_o$  at each layer. In Section 5, we collect Jacobians within Mamba to test the linearity of relational encodings as done by Hernandez et al. (2023). And in Section 6 we address the challenge of applying attention patching in Mamba, as used in Geva et al. (2023) to isolate information flow in GPT LMs.

### 3 Locating Key States for Factual Recall

We begin with activation patching, seeking to understand if there are specific hidden states which play important roles during factual recall. We select a fact  $(s, r, o)$  that the LM knows, where  $r$  is a relation that associates a subject entity  $s$  with an object entity  $o$ . To estimate each state’s contribution towards a correct factual prediction ( $s = \textit{Michael Jordan}$ ,  $r = \textit{professionally played}$ ,  $o = \textit{basketball}$ ), we collect model activations across three different runs:

**clean run**  $G$ : In the clean run, we simply run the model on a prompt specifying the fact we are interested in. For example,  $x = (s, r) = \textit{Michael Jordan professionally played}$ . We cache all the hidden states during the clean run to be used later:  $\{h_i^{(\ell)}, a_i^{(\ell)}, s_i^{(\ell)}, g_i^{(\ell)} \mid i \in [1, T], \ell \in [1, L]\}$ .

**corrupted run**  $G^*$ : In the corrupted run, we swap  $s$  with a different subject  $s^*$  (*Pelé*) such that the LM gives a different answer  $o^*$  (*soccer*) to the modified prompt  $x^* = (s^*, r)$  (i.e.,  $o^* \neq o$ ).

This subject-swapping approach follows the recommendation of Zhang & Nanda (2023) and has the advantage of using a natural text perturbations to avoid introducing out-of-domain states to the

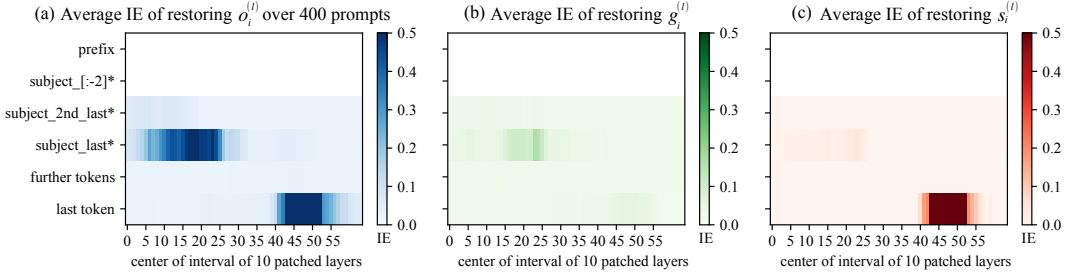


Figure 3: Average indirect effect of different states  $o_i^{(\ell)}$ ,  $g_i^{(\ell)}$ , and  $s_i^{(\ell)}$  over 400 facts. For each layer  $\ell$ , states for a window of 10 layers around  $\ell$  are restored from the clean run  $G$ .

model’s computation, as may happen with corrupting  $s$  embeddings with Gaussian noise (used in Meng et al. (2022a)).

**patched run**  $G^*[\leftarrow h_i^{(\ell)}]$ : In the patched run, we run the model on the corrupted prompt  $x^*$ , but intervene on  $h_i^{(\ell)}$  by replacing its value with the corresponding state cached from the clean run  $G$ . The remainder of the computation is run normally, meaning that the patched state can have a downstream effect of potentially changing all the states that depend on it. See Figure 2a.

Let  $p(o)$ ,  $p^*(o)$ , and  $p^*[\leftarrow h_i^{(\ell)}](o)$  denote the probability assigned to the correct answer  $o$  in  $G$ ,  $G^*$ , and  $G^*[\leftarrow h_i^{(\ell)}]$  respectively. To measure the contribution of  $h_i^{(\ell)}$  in recalling the fact  $(s, r, o)$ , we define the *indirect effect* (IE) as:

$$\text{IE}_{h_i^{(\ell)}} = \frac{p^*[\leftarrow h_i^{(\ell)}](o) - p^*(o)}{p(o) - p^*(o)} \quad (7)$$

In Figure 2b we plot the average indirect effect of restoring the residual states  $h_i^{(\ell)}$  across different layer-token positions over 400 facts. The high IE in later layers at the last token position is natural, as restoring a clean  $h_i^{(\ell)}$  there means restoring most of the model computation from  $G$ . However, Mamba also shows high causality in the middle layers at the last subject token position. This is consistent with what Meng et al. (2022a) observed in GPT family of language models.

In Figure 3 we plot the average IE for  $o_i^{(\ell)}$ ,  $g_i^{(\ell)}$ , and  $s_i^{(\ell)}$ . The plot for  $o_i^{(\ell)}$  (Figure 3a) looks very similar to Figure 2b, confirming that the output from MambaBlock has strong causal effects at both early and late sites. Interestingly, Figure 3c shows that the selective-SSM output  $s_i^{(\ell)}$  has high IE in later layers at the last token of the prompt, resembling the behavior of attention modules in GPT models (Meng et al., 2022a). However, there is no state that appears to do the opposite; in other words, there is no state with strong effects at the early site and not at the late site. (The gate output  $g_i^{(\ell)}$  does have stronger IE at the early site than the late site, but the effects are very weak.) A comparison with the comparable Pythia-2.8b transformer LMs is shown in Figure 9 in Appendix C. This comparison reveals a key way that Mamba differs from transformers: while transformer MLP outputs have effects in the early site and not the late site, in Mamba there is no similar state that specializes only at the early site at which factual recall would be expected to occur. This presents the question: which parameters in Mamba mediate factual recall?

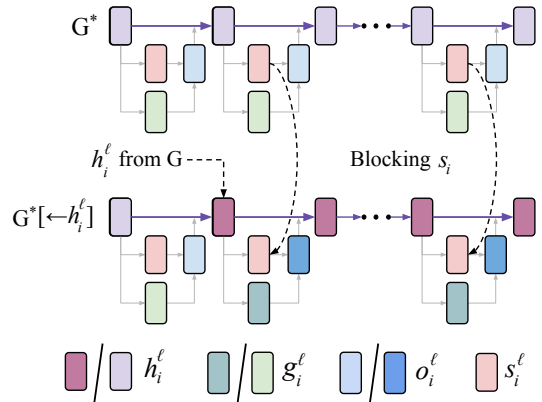


Figure 4: A probe for path-specific effects.  $h_i^{(\ell)}$  is restored from the clean run  $G$  as in Figure 2a. Then, to reveal the role of the SSM component,  $s_i$  states from the corrupted run  $G^*$  are also patched to block the prevent contributions on the  $s_i$  paths.

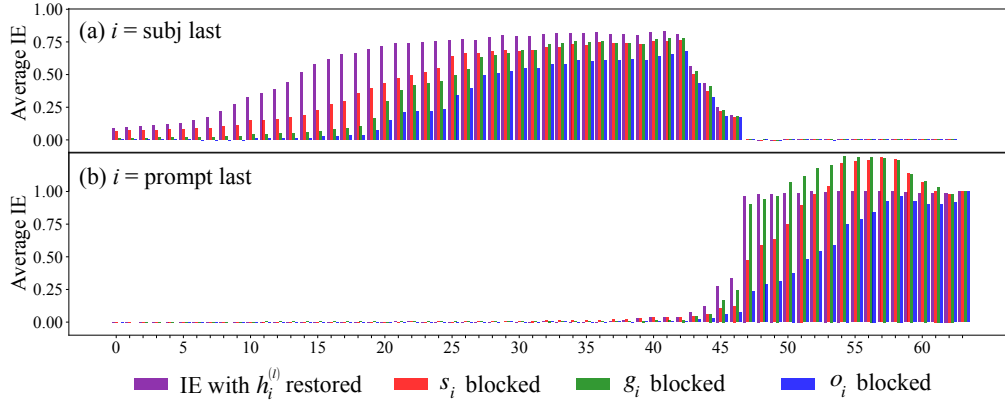


Figure 5: Impact of ablating  $s_i$ ,  $g_i$ , and  $o_i$  on  $\text{IE}_{h_i^{(\ell)}}$  for (a) *subject last* and (b) *prompt last* token positions. Taken together (a) and (b) show a clear separation roles between early-mid and later layers in Mamba-2.8b.  $h_i^{(\ell)}$  up to layer 46 only show strong IE at the subject last token position and have negligible impact after that. Whereas IE of  $h_i^{(\ell)}$  jumps to 1.0 after layer 46. (a) also shows that, at the subject last token, before layer 27 – 28,  $\text{IE}_{h_i^{(\ell)}}$  is significantly reduced by blocking either  $o_i$ ,  $g_i$ , or  $s_i$  paths (sorted in descending order of damaging  $\text{IE}_{h_i^{(\ell)}}$ ). (b) At the prompt last token, ablating  $o_i$  or  $s_i$  paths can significantly reduce  $\text{IE}_{h_i^{(\ell)}}$  in layers 47 – 50.

To investigate this question, we replicate an experiment from Meng et al. (2022a) to probe *path-specific effects* (Pearl, 2022) for paths that avoid either  $g_i$ ,  $s_i$ , or  $o_i$  contributions. First, in the corrupted run  $G^*$ , at token position  $i$ , we cache all the contributions from the  $s_i$  paths as  $s_i^* = \{s_i^{*(\ell)} \mid \ell \in [1, L]\}$ . Then in the patched run  $G^*[\leftarrow h_i^{(\ell)}]$  we patch  $h_i^{(\ell)}$  cached from the clean run  $G$  into its corresponding state (as in Figure 2a), but with an additional modification: to understand the contribution from the  $s_i$  paths, we sever those paths by patching  $s_i^*$  to their corresponding locations (see Figure 4). The same experiment can be conducted to understand the contributions of  $g_i$  and  $o_i$ . We note that blocking the  $o_i$  paths will block the  $s_i$  and  $g_i$  paths as well (see Figure 1).

In Figure 5 we plot the average results of this experiment done at token positions (a)  $i = \text{subject last}$  and (b)  $i = \text{prompt last}$  over 400 examples. The key findings can be understood by examining the gap between the purple bars and the green, red, and blue bars: a large gap indicates a strong mediating role for SSM,  $W_g$ , or  $W_o$  parameters, respectively. At the early site at the subject last token, both SSM and  $W_g$  have a strong role, but  $W_o$  plays an even larger role. Yet the strongest mediator at the late site is also  $W_o$ . This experiment highlights the importance of  $W_o$  in both stages of predicting a fact, but it also suggests that Mamba does not separate early-site factual recall between these groups of parameters as cleanly as transformers. However, Figure 5 reveals a clean separation of roles between early to mid and later layers, similar to what Hernandez et al. (2023) observed in transformer LMs. However, we note that this division of responsibilities between layers can be more sharply noticed in Mamba when compared to transformers LMs (compare with Figure 10).

## 4 Editing Facts With ROME

Having begun to characterize the locations of important states for factual recall, we now investigate whether factual recall behavior can be edited. In particular, we apply the ROME (Rank One Model Editing, Meng et al., 2022a) technique to Mamba. ROME begins with the observation that any linear transformations can be considered as an associative memory (Anderson, 1972; Kohonen, 1972), mapping a set of keys  $K = [k_1|k_2|\dots]$  to their corresponding values  $V = [v_1|v_2|\dots]$ , and uses this to edit factual associations in transformer LMs. Here, we apply the technique to a particular set of linear transformations within Mamba, and report our editing success on each.<sup>2</sup>

The input to ROME is a prompt  $x = (s, r)$ , where  $s$  (*Emmanuel Macron*) is a subject entity and  $r$  (*is the President of*) is a relation. ROME also takes a counterfactual object  $o^*$  (*England*), meant to

<sup>2</sup>Further motivating these experiments, previous work has shown that the locations identified by activation patching techniques are often not those which have the strongest edit performance (Hase et al., 2024).

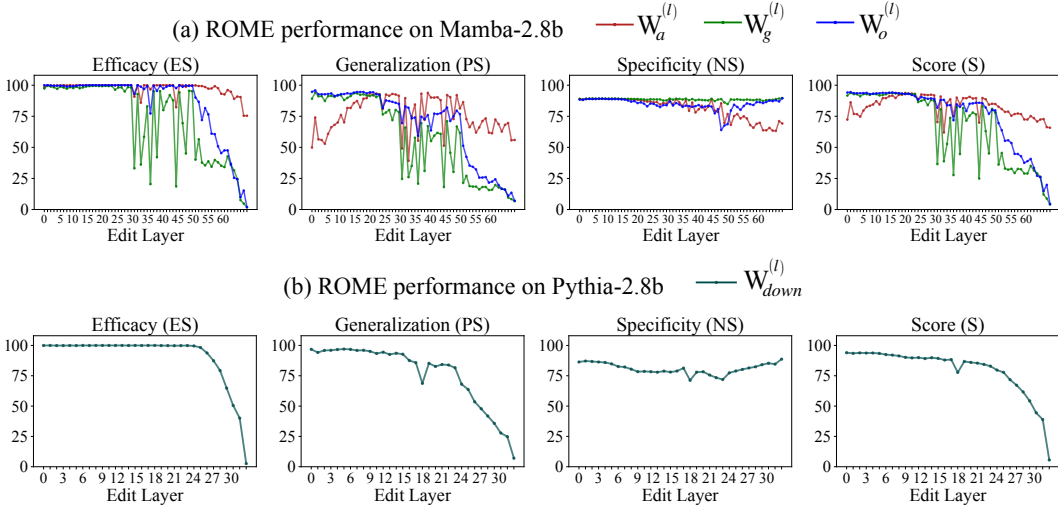


Figure 6: ROME performance in editing facts across different layers **(a)** by modifying  $W_a^{(\ell)}$ ,  $W_g^{(\ell)}$ ,  $W_o^{(\ell)}$  in Mamba-2.8b, and **(b)** modifying  $W_{down}^{(\ell)}$  in Pythia-2.8b. Results are reported on the first 2000 examples in the COUNTERFACT dataset.

replace the correct object  $o$  (*France*) in the model’s output. To effect that change, ROME generates a rank-one update to  $W_{down}^{(\ell)}$ , the down-projection matrix of the MLP module for the last token of the subject at layer  $\ell$ —which plays the role of the associative memory. In generating the rank-one update, ROME considers the input to  $W_{down}^{(\ell)}$  as the *key* ( $k_*$ ). Then, with gradient descent ROME calculates a *value* ( $v_*$ ) such that, when  $v_*$  is inserted as the output of  $W_{down}^{(\ell)}$ , the model will output  $o^*$ . Importantly, while optimizing  $v_*$ , ROME attempts to minimize unrelated changes in model outputs (*Joe Biden*, for example, should still be mapped to *the United States* post-edit). Finally, ROME adds a rank-1 matrix  $\Delta$  to  $W_{down}^{(\ell)}$  such that  $(W_{down}^{(\ell)} + \Delta)k_* \approx v_*$ . (For mathematical and implementation details see Meng et al. (2022a).)

#### 4.1 Applying ROME in Mamba

We apply ROME to three different projection matrices:  $W_a^{(\ell)}$  which affects only the selective-SSM path,  $W_g^{(\ell)}$  which affects only the gating path, and  $W_o^{(\ell)}$ , the final output of the MambaBlock, which is added to the residual. We plot ROME performance across different layers and projection matrices ( $W_a^{(\ell)}$ ,  $W_g^{(\ell)}$ , and  $W_o^{(\ell)}$ ) in Figure 6a.

To evaluate editing performance, we use the COUNTERFACT dataset from Meng et al. (2022a). COUNTERFACT contains 20K counterfactual examples in the form  $(s, r, o \rightarrow o^*)$ , where  $o$  is the correct answer to the prompt  $x = (s, r)$ , and  $o^*$  is the object which is to be inserted as the new answer to the prompt. (See Appendix A.1 for details). We select the first 2000 examples from this dataset for our module-layer sweep. We use the original evaluation matrices in Meng et al. (2022a) to measure ROME edit performance.

The final **score (S)** in the ROME evaluation suite is the harmonic mean of three different scores:

1. **Efficacy (ES)**: For an edit request  $(s, r, o \rightarrow o^*)$ , we say the edit is *effective* if, post-edit, the LM assigns  $p(o^*) > p(o)$  in response to the prompt  $x = (s, r)$ . Efficacy reflects the portion of the examples where the edit was effective.
2. **Generalization (PS)**: A successful edit should be persistent across different paraphrases of  $(s, r)$ . For each of the request instances  $(s, r, o \rightarrow o^*)$ ,  $p(o^*) > p(o)$  is checked post-edit with a set of different rephrasings  $x_p \sim \mathcal{P}(s, r)$  of the prompt  $x = (s, r)$ , where  $\mathcal{P}$  denotes a set of paraphrased templates for the relation  $r$ .

3. **Specificity (NS)**: Finally, the edit should be specific to  $\mathcal{P}(s, r)$  and should not additionally change the mapping of some nearby subject  $s_n$  to  $o^*$ . To evaluate the specificity of an edit we measure  $p(o_n) > p(o^*)$  with  $\mathcal{P}(s_n, r)$  for a set of nearby factual associations  $\{(s_n, r, o_n) \mid o_n \neq o^*\}$ .

Figure 6a shows that ROME can achieve high scores (S) for a range of early to middle layers by modifying any one of the projection matrices  $W_a^{(\ell)}$ ,  $W_g^{(\ell)}$ , or  $W_o^{(\ell)}$ , matching observations made by Hase et al. (2024) regarding transformer LMs. However, performance does depend on the location of the edit. For example, in the case of  $W_g^{(\ell)}$  and  $W_o^{(\ell)}$ , the score (S) and generalization (PS) drops after layer 43. This is consistent with our findings from the path-blocking experiment in Figure 5a. We also find that edits to  $W_a^{(\ell)}$  have poor generalization (PS) in early layers, whereas high PS can be achieved at early layers by modifying either  $W_g^{(\ell)}$  or  $W_o^{(\ell)}$ , consistent with their higher indirect effects as seen in Figure 5a.

Where is the right place to apply ROME on Mamba? Figure 3 could suggest  $W_g^{(\ell)}$ , since the causal effect of  $g_i$  states is mostly concentrated at the subject last token, similar to the behavior of MLPs in transformers (Meng et al., 2022a). Consistent with this is the architectural fact that, just as transformers’  $W_{down}^{(\ell)}$  connects to attention modules only through the residual stream, the output of  $W_g^{(\ell)}$  does not flow through the Conv + SSM module—a module that other work has suggested might play role similar to that played by attention heads in transformers (Grazzi et al., 2024). And, indeed, we find that ROME can successfully insert facts by modifying  $W_g^{(\ell)}$ . On the other hand Figure 6a reveals sudden drops in efficacy and generalization at middle layer gates, suggesting that  $W_g^{(\ell)}$  may be an unreliable mediator at some layers. Our experiments further show that the best performance for ROME is empirically achieved by modifying  $W_o^{(\ell)}$ . This is consistent with the fact that  $o_i$  states show a stronger causal effect at the subject last token than  $g_i$  states do (see Figure 3a). Additionally, ROME achieves better generalization (PS), competitive specificity (NS), and an overall better score (S) with  $W_o^{(\ell)}$ . We hypothesize that the strong performance of  $W_o^{(\ell)}$  may be due to the the separation of roles between early-mid and later layers observed in Figures 2b, 3a, and 5. Also see Appendix B where we isolate the contribution of  $W_o^{(\ell)}$  by subtracting  $\text{IE}_{s_i^{(\ell)}} + \text{IE}_{g_i^{(\ell)}}$  from  $\text{IE}_{o_i^{(\ell)}}$ , which reveal a critical role of  $W_o^{(\ell)}$  in early-mid layers at subject last token position while mediating a fact.

We plot ROME performance for a similar sized Pythia model on Figure 6b for comparison.

## 5 LINEARITY OF RELATION EMBEDDING (LRE)

With activation patching we can identify *where* facts are located inside a LM. We are also interested in understanding *how* LM extracts this information given  $x = (s, r)$ . Figures 2b and 5 show a clear separation of roles in early-mid and later layers in Mamba. We observe a similar phenomena in autoregressive transformer LMs (Meng et al., 2022a;b; Geva et al., 2023). According to Geva et al. (2023), in transformer LMs, the subject entity representation  $\mathbf{s}$ , at the subject last token position, goes through an *enrichment* process, mediated by the MLP in the early-mid layers, where  $\mathbf{s}$  is populated with different facts/attributes relevant to the subject entity  $s$ . And, then at the last token position attention modules perform a *query* in the *enriched*  $\mathbf{s}$  to extract the answer to the prompt  $x = (s, r)$ . Hernandez et al. (2023) approximate the *query* performed in the *enriched*  $\mathbf{s}$  for a specific relation  $r$  by taking the first order Taylor series approximation (LRE) of the LM computation  $F$  as -

$$F(\mathbf{s}, r) \approx \beta \mathbf{J}_\rho \mathbf{s} + b$$

$$\text{where } \mathbf{J} = \mathbb{E}_{\mathbf{s}_i, r} \left[ \frac{\partial F}{\partial \mathbf{s}} \Big|_{(\mathbf{s}_i, r)} \right], \quad b = \mathbb{E}_{\mathbf{s}_i, r} \left[ F(\mathbf{s}, r) - \frac{\partial F}{\partial \mathbf{s}} \mathbf{s} \Big|_{(\mathbf{s}_i, r)} \right], \quad (8)$$

$\beta$  is a scalar, and  $\rho$  is the rank of  $\mathbf{J}$

Hernandez et al. (2023) show that for a range of different relations it is possible to achieve a LRE that is faithful to the model computation  $F$  by averaging the approximations of  $\mathbf{J}$  and  $b$  calculated on just  $n = 5$  examples. We utilize LRE to understand the complexity of decoding *factual* relations in

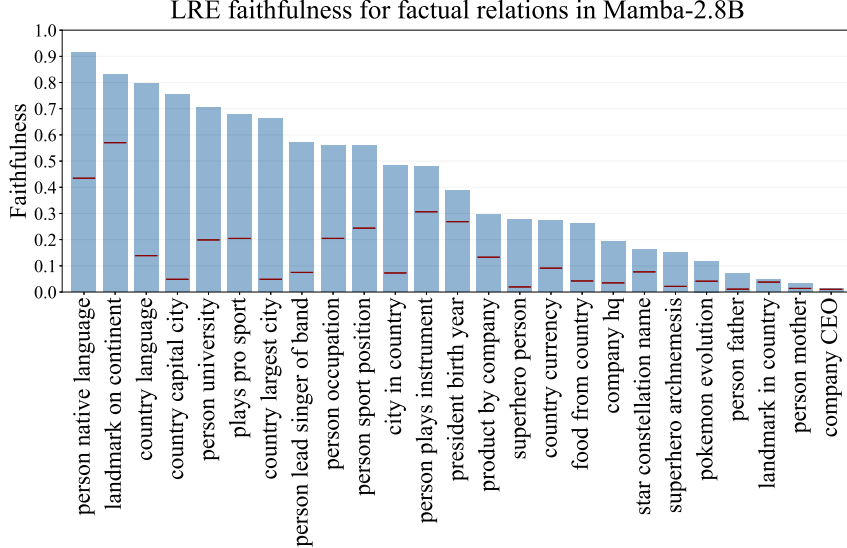


Figure 7: LRE *faithfulness* with  $n = 5$  samples for all the factual relations. Horizontal red lines indicate random choice baseline (in the RELATIONS dataset).

Mamba. We find the hyperparameters  $\beta$ ,  $\rho$  and the layer  $\ell$  (where to extract enriched  $\mathbf{s}$  from) using grid search. For mathematical and implementation details, see Hernandez et al. (2023).

We plot the *faithfulness* of LRE with  $n = 5$  samples on Figure 7. *faithfulness* represents the portion of facts in  $r$  that can be correctly retrieved if the LM computation  $F(\mathbf{s}, r)$  is replaced with  $LRE(\mathbf{s})$ .

We only calculate LRE for the *factual* relations in the RELATIONS dataset. Figure 7 shows that only for 10 out of 26 factual relations a *linear* LRE can achieve more than 50% *faithfulness*. For comparison, in the same sized Pythia-2.8b LRE achieves  $> 50\%$  *faithfulness* for 11 factual relations (see Appendix E). And, in both Mamba and Pythia, LRE fails to achieve good *faithfulness* for the relations where the *range* (the number of unique answers) is larger.

## 6 Attention Knock-out in Mamba?

In transformer LMs, attention modules bring information from the other token positions. Each of the attention heads in an attention module  $attn^{(\ell)}$  calculates an *attention matrix*  $L$ , where  $L_{k,q}$  quantifies how much attention is being paid to the  $q^{th}$  token by the  $k^{th}$  token. See Vaswani et al. (2017) for details on the attention operation. We can block information flow from  $q^{th}$  token to  $k^{th}$  via a specific attention head by simply setting  $L_{k,q} := -\infty$  in the forward pass. This patch-dependent attention blocking (or attention “*knock-out*”) is also a form of causal mediation analysis and it has been effective in understanding the information flow in transformer LMs (Geva et al., 2023; Wang et al., 2022; Todd et al., 2023).

For Mamba, Ali et al. (2024) show that the amount of information retained in the  $k^{th}$  token state  $s_k^{(\ell)}$ , from the *convolved* state at  $q^{th}$  token  $c_q^{(\ell)}$  (where  $q < k$ ), after the selective-SSM operation (see Equations 4 and 5) can be visualized as an *attention matrix* per channel (dim). Since the selective-SSM operation is linear, the information retained in  $s_k^{(\ell)}$  from  $c_q^{(\ell)}$  can be calculated accurately as  $\tilde{\alpha}_{k,q} = \bar{C}_k^{(\ell)} \left( \prod_{i=q+1}^k \bar{A}_i^{(\ell)} \right) \bar{B}_q^{(\ell)} c_q^{(\ell)}$ , where  $\bar{A}_i^{(\ell)}$ ,  $\bar{B}_i^{(\ell)}$ , and  $\bar{C}_i^{(\ell)}$  are input-dependent parameters for the  $i^{th}$  token. See Gu & Dao (2023) and Ali et al. (2024) for details. We ask: can we block the information flow from the  $q^{th}$  token to the  $k^{th}$  token in Mamba by subtracting out  $\tilde{\alpha}_{k,q}$  from  $s_k^{(\ell)}$ ? If so, attention knockout experiments in Mamba become feasible.

**We find that blocking information flow from the  $q^{th}$  token to the  $k^{th}$  token in the Conv + SSM operation can be difficult.** Note that, since  $c_q^{(\ell)}$  is a *convolved* state with a receptive field of size 4 in Mamba-2.8b, the states  $c_{q+1}^{(\ell)}$ ,  $c_{q+2}^{(\ell)}$ , and  $c_{q+3}^{(\ell)}$  retain information from  $a_q^{(\ell)}$ . And, these states can “*leak*” information about  $a_q^{(\ell)}$  to  $s_k^{(\ell)}$ . To stop this leakage, we would want to subtract from  $s_k^{(\ell)}$  all



the information retained about  $a_q^{(\ell)}$ . However, calculating this is challenging because of the SiLU non-linearity after Conv1D (see Equation (4)).

In Appendix D, we present a version of attention knock-out experiment, where we block information flow of the  $q^{th}$  token to *all* the future tokens with Conv + SSM operation. We recognize that this intervention is not as *surgical* as blocking information from  $q^{th}$  token to just  $k^{th}$  token. However, with some caveats, this experiment leads us to draw some conclusion about the information flow in Mamba that is similar to what Geva et al. (2023) found for GPT LMs. See Appendix D for details.

## 7 Related Works

**Mamba.** Mamba is a recent family of language models that are based on state space models (SSMs). Neural SSM-based models have achieved good performance across different modalities, including vision (Nguyen et al., 2022), audio (Goel et al., 2022), and genomic sequences (Nguyen et al., 2023). Only recently, however, with Mamba, have they become competitive with the language modeling performance of transformers (Gu & Dao, 2023). Like transformers, Mamba contains factual knowledge about real world entities (Grazzi et al., 2024). However, knowledge representation in Mamba (and other LMs based on SSMs) has up to now remained unexplored.

There are few works focused on interpreting Mamba. Ali et al. (2024) identify implicit attention-like matrices formed by Mamba’s selective state space layers. Grazi et al. (2024), while not strictly focused on interpreting Mamba’s internals, apply linear probes to Mamba’s (decoded) intermediate states during in-context regression tasks. Like us, they find substantial similarities between Mamba and transformer models: both architectures pursue “iterative” strategies, with the task loss falling more or less monotonically as the layer index increases.

**Locating Factual Knowledge in Language Models.** To make factually correct statements about the world a LM has to store factual knowledge about real world entities somewhere in its parameters. Understanding how and where a neural network stores knowledge is a core problem for interpretability and it has thus been studied from several perspectives (Ji et al., 2021; Wang et al., 2014). One line of work trains classifiers to probe for properties encoded in model representations (Ettinger et al., 2016; Shi et al., 2016; Hupkes et al., 2018; Conneau et al., 2018; Belinkov et al., 2017; Belinkov & Glass, 2019). However, the flexibility of these classifiers can lead to overestimating model knowledge and capabilities (Belinkov, 2022). Causal mediation analysis methods (Pearl, 2022) attempt to measure the causal contribution of intermediate states to task performance. Meng et al. (2022a;b) use activation patching to identify key MLP modules for factual recall, highlighting the middle layers at particular token positions as being especially important. Similarly, Geva et al. (2023) apply causal mediation analysis to attention modules, seeking to understand the mechanism of cross-token factual information flow inside transformer LMs.

## 8 Discussion

In this paper we have explored whether the analytical methods and tools developed for transformer LMs can also be applied on Mamba, a recurrent state-space architecture, and we have compared the mechanisms of factual recall between the two classes of models. Our experiments have been limited to Mamba-2.8b, the largest available LM of that family, and comparisons to Pythia-2.8b (selected over Llama or GPT models as they do not offer pretrained models of similar size).

With activation patching we have found that, similar to autoregressive transformer LMs, Mamba shows signs of localization at the last subject token and at specific layer ranges while recalling a fact. We have applied rank-one model editing (ROME) to rewrite a fact in specific parameters in Mamba. Although, unlike transformers, Mamba has no MLP modules, we find that their  $W_o$  weights can receive edits with good generalization and specificity at a range of layers. Then we have studied the linearity of the embeddings of factual relations in Mamba and have found that many can be well approximated by LRE, again resembling transformer LMs. Although Mamba has no attention modules, we have been able to partially adapt the tools of attention knock-out using an SSM blocking technique, and this reveals information flows similar to transformers. In summary, we find that many of the tools used to interpret and edit large transformers can be adapted to work with Mamba as well, and that despite the architectural differences, when it comes to factual recall, Mamba shares many similarities with transformer LMs.

## Ethics

By exploring the factual recall mechanism in Mamba, we potentially improve its transparency, enabling oversight and control. However, the ability to modify facts directly in the model brings with it the potential for abuse, such as adding malicious misinformation or bias.

## Reproducibility

We ran all experiments on workstations with either 80GB NVIDIA A100 GPUs or 48GB A6000 GPUs, using the HuggingFace Transformers library (Wolf et al., 2019) and PyTorch (Paszke et al., 2019). We make use of publicly available datasets COUNTERFACT and RELATIONS in this work. We will make our source code open source after the anonymity period has ended.

## References

- Ameen Ali, Itamar Zimmerman, and Lior Wolf. The hidden attention of mamba models. *arXiv preprint arXiv:2403.01590*, 2024.
- James A Anderson. A simple neural network generating an interactive memory. *Mathematical biosciences*, 14(3-4):197–220, 1972.
- Yonatan Belinkov. Probing classifiers: Promises, shortcomings, and advances. *Computational Linguistics*, 48(1):207–219, 2022.
- Yonatan Belinkov and James Glass. Analysis methods in neural language processing: A survey. *Transactions of the Association for Computational Linguistics*, 7:49–72, 2019.
- Yonatan Belinkov, Nadir Durrani, Fahim Dalvi, Hassan Sajjad, and James Glass. What do neural machine translation models learn about morphology? *arXiv preprint arXiv:1704.03471*, 2017.
- Stella Biderman, Hailey Schoelkopf, Quentin Gregory Anthony, Herbie Bradley, Kyle O’Brien, Eric Hallahan, Mohammad Aflah Khan, Shivanshu Purohit, USVSN Sai Prashanth, Edward Raff, et al. Pythia: A suite for analyzing large language models across training and scaling. In *International Conference on Machine Learning*, pp. 2397–2430. PMLR, 2023.
- Kyunghyun Cho, Bart Van Merriënboer, Dzmitry Bahdanau, and Yoshua Bengio. On the properties of neural machine translation: Encoder-decoder approaches. *arXiv preprint arXiv:1409.1259*, 2014.
- Alexis Conneau, German Kruszewski, Guillaume Lample, Loïc Barrault, and Marco Baroni. What you can cram into a single vector: Probing sentence embeddings for linguistic properties. *arXiv preprint arXiv:1805.01070*, 2018.
- James Durbin and Siem Jan Koopman. *Time series analysis by state space methods*, volume 38. OUP Oxford, 2012.
- Yanai Elazar, Nora Kassner, Shauli Ravfogel, Abhilasha Ravichander, Eduard Hovy, Hinrich Schütze, and Yoav Goldberg. Measuring and improving consistency in pretrained language models. *Transactions of the Association for Computational Linguistics*, 9:1012–1031, 2021.
- Allyson Ettinger, Ahmed Elgohary, and Philip Resnik. Probing for semantic evidence of composition by means of simple classification tasks. In *Proceedings of the 1st workshop on evaluating vector-space representations for nlp*, pp. 134–139, 2016.
- Atticus Geiger, Zhengxuan Wu, Hanson Lu, Josh Rozner, Elisa Kreiss, Thomas Icard, Noah D. Goodman, and Christopher Potts. Inducing causal structure for interpretable neural networks. *CoRR*, abs/2112.00826, 2021. URL <https://arxiv.org/abs/2112.00826>.
- Mor Geva, Jasmijn Bastings, Katja Filippova, and Amir Globerson. Dissecting recall of factual associations in auto-regressive language models. *arXiv preprint arXiv:2304.14767*, 2023.

- Karan Goel, Albert Gu, Chris Donahue, and Christopher Re. It’s raw! Audio generation with state-space models. In Kamalika Chaudhuri, Stefanie Jegelka, Le Song, Csaba Szepesvari, Gang Niu, and Sivan Sabato (eds.), *Proceedings of the 39th International Conference on Machine Learning*, volume 162 of *Proceedings of Machine Learning Research*, pp. 7616–7633. PMLR, 17–23 Jul 2022. URL <https://proceedings.mlr.press/v162/goel22a.html>.
- Riccardo Grazi, Julien Siems, Simon Schrodi, Thomas Brox, and Frank Hutter. Is Mamba Capable of In-Context Learning?, 2024. URL <http://arxiv.org/abs/2402.03170>.
- Albert Gu and Tri Dao. Mamba: Linear-time sequence modeling with selective state spaces. *arXiv preprint arXiv:2312.00752*, 2023.
- Albert Gu, Karan Goel, and Christopher Ré. Efficiently modeling long sequences with structured state spaces. *arXiv preprint arXiv:2111.00396*, 2021.
- Peter Hase, Mohit Bansal, Been Kim, and Asma Ghandeharioun. Does localization inform editing? surprising differences in causality-based localization vs. knowledge editing in language models. *Advances in Neural Information Processing Systems*, 36, 2024.
- Evan Hernandez, Arnab Sen Sharma, Tal Haklay, Kevin Meng, Martin Wattenberg, Jacob Andreas, Yonatan Belinkov, and David Bau. Linearity of relation decoding in transformer language models. *arXiv preprint arXiv:2308.09124*, 2023.
- Sepp Hochreiter and Jürgen Schmidhuber. Long short-term memory. *Neural computation*, 9(8): 1735–1780, 1997.
- Dieuwke Hupkes, Sara Veldhoen, and Willem Zuidema. Visualisation and diagnostic classifiers’ reveal how recurrent and recursive neural networks process hierarchical structure. *Journal of Artificial Intelligence Research*, 61:907–926, 2018.
- Shaoxiong Ji, Shirui Pan, Erik Cambria, Pekka Marttinen, and S Yu Philip. A survey on knowledge graphs: Representation, acquisition, and applications. *IEEE Transactions on Neural Networks and Learning Systems*, 33(2):494–514, 2021.
- Teuvo Kohonen. Correlation matrix memories. *IEEE transactions on computers*, 100(4):353–359, 1972.
- Siem Jan Koopman, Neil Shephard, and Jurgen A Doornik. Statistical algorithms for models in state space using ssfpack 2.2. *The Econometrics Journal*, 2(1):107–160, 1999.
- Kevin Meng, David Bau, Alex Andonian, and Yonatan Belinkov. Locating and editing factual associations in gpt. *Advances in Neural Information Processing Systems*, 35:17359–17372, 2022a.
- Kevin Meng, Arnab Sen Sharma, Alex Andonian, Yonatan Belinkov, and David Bau. Mass-editing memory in a transformer. *arXiv preprint arXiv:2210.07229*, 2022b.
- Neel Nanda, Senthooan Rajamanoharan, János Kramár, and Rohin Shah. Fact finding: Attempting to reverse-engineer factual recall on the neuron level, 2023. URL <https://www.lesswrong.com/posts/iGuwZTHWb6DFY3sKB/fact-finding-attempting-to-reverse-engineer-factual-recall>.
- Eric Nguyen, Karan Goel, Albert Gu, Gordon Downs, Preety Shah, Tri Dao, Stephen Baccus, and Christopher Ré. S4nd: Modeling images and videos as multidimensional signals with state spaces. In S. Koyejo, S. Mohamed, A. Agarwal, D. Belgrave, K. Cho, and A. Oh (eds.), *Advances in Neural Information Processing Systems*, volume 35, pp. 2846–2861. Curran Associates, Inc., 2022. URL [https://proceedings.neurips.cc/paper\\_files/paper/2022/file/13388efc819c09564c66ab2dc8463809-Paper-Conference.pdf](https://proceedings.neurips.cc/paper_files/paper/2022/file/13388efc819c09564c66ab2dc8463809-Paper-Conference.pdf).
- Eric Nguyen, Michael Poli, Marjan Faizi, Armin Thomas, Callum Birch-Sykes, Michael Wornow, Aman Patel, Clayton Rabideau, Stefano Massaroli, Yoshua Bengio, Stefano Ermon, Stephen A. Baccus, and Chris Ré. Hyenadna: Long-range genomic sequence modeling at single nucleotide resolution, 2023.

- Adam Paszke, Sam Gross, Francisco Massa, Adam Lerer, James Bradbury, Gregory Chanan, Trevor Killeen, Zeming Lin, Natalia Gimelshein, Luca Antiga, et al. Pytorch: An imperative style, high-performance deep learning library. *Advances in neural information processing systems*, 32, 2019.
- Judea Pearl. Direct and indirect effects. In *Probabilistic and causal inference: the works of Judea Pearl*, pp. 373–392. 2022.
- Xing Shi, Inkit Padhi, and Kevin Knight. Does string-based neural mt learn source syntax? In *Proceedings of the 2016 conference on empirical methods in natural language processing*, pp. 1526–1534, 2016.
- Eric Todd, Millicent L Li, Arnab Sen Sharma, Aaron Mueller, Byron C Wallace, and David Bau. Function vectors in large language models. *arXiv preprint arXiv:2310.15213*, 2023.
- Ashish Vaswani, Noam Shazeer, Niki Parmar, Jakob Uszkoreit, Llion Jones, Aidan N Gomez, Łukasz Kaiser, and Illia Polosukhin. Attention is all you need. *Advances in neural information processing systems*, 30, 2017.
- Jesse Vig, Sebastian Gehrmann, Yonatan Belinkov, Sharon Qian, Daniel Nevo, Yaron Singer, and Stuart Shieber. Investigating gender bias in language models using causal mediation analysis. In H. Larochelle, M. Ranzato, R. Hadsell, M.F. Balcan, and H. Lin (eds.), *Advances in Neural Information Processing Systems*, volume 33, pp. 12388–12401. Curran Associates, Inc., 2020. URL [https://proceedings.neurips.cc/paper\\_files/paper/2020/file/92650b2e92217715fe312e6fa7b90d82-Paper.pdf](https://proceedings.neurips.cc/paper_files/paper/2020/file/92650b2e92217715fe312e6fa7b90d82-Paper.pdf).
- Kevin Wang, Alexandre Variengien, Arthur Conmy, Buck Shlegeris, and Jacob Steinhardt. Interpretability in the wild: a circuit for indirect object identification in gpt-2 small. *arXiv preprint arXiv:2211.00593*, 2022.
- Zhen Wang, Jianwen Zhang, Jianlin Feng, and Zheng Chen. Knowledge graph embedding by translating on hyperplanes. In *Proceedings of the AAAI conference on artificial intelligence*, volume 28, 2014.
- Thomas Wolf, Lysandre Debut, Victor Sanh, Julien Chaumond, Clement Delangue, Anthony Moi, Pierric Cistac, Tim Rault, Rémi Louf, Morgan Funtowicz, et al. Huggingface’s transformers: State-of-the-art natural language processing. *arXiv preprint arXiv:1910.03771*, 2019.
- Fred Zhang and Neel Nanda. Towards best practices of activation patching in language models: Metrics and methods. *arXiv preprint arXiv:2309.16042*, 2023.

## A Datasets

We use two datasets; COUNTERFACT by Meng et al. (2022a) and RELATIONS by Hernandez et al. (2023) in this work.

### A.1 COUNTERFACT

Meng et al. (2022a) developed the COUNTERFACT dataset for evaluating the efficacy of counterfactual edits in language models. It was prepared by adapting PARAREL (Elazar et al. (2021)) and scraping Wikidata. The dataset contains 21,919 requests  $\{s, r, o, o^*, \pi^*\}$  where  $o$  is the correct answer to the prompt  $x = (s, r)$ ,  $o^*$  is the counterfactual edit request, and  $\pi^* \sim \mathcal{P}(s, r)$  is a paraphrase of the prompt  $x = (s, r)$  to test for generalizability (PS). Each of the records also contain some neighborhood prompts  $\pi_N$  to test for specificity (NS) and some generation prompts  $\pi_G$  to test if LM generation post-edit is fluent and consistent with the edit. Please refer to Meng et al. (2022a) for details on the curation of this dataset.

We evaluate ROME performance in Mamba-2.8b and Pythia-2.8b on the first 2000 records from COUNTERFACT.

### A.2 RELATIONS

The RELATIONS dataset introduced in Hernandez et al. (2023) consists of 47 relations of 4 types; *factual*, *linguistic*, *bias*, and *commonsense*. A relation  $r$  is an association between two entities. For example, the relation,  $r = \text{professionally played the sport}$  connects the subject  $s = \text{Michael Jordan}$  with the object  $o = \text{basketball}$ . The dataset contains a set of  $(s, o)$  for each relation  $r$ .

In the scope of this paper, we only utilize the 26 *factual* relations from this dataset. We evaluate LRE in Mamba and Pythia for all the 26 factual relations. We also use this dataset for locating key fact-differentiating states in Section 3 and Appendix C. We randomly sample 400 examples  $(s, r, o)$  across 6 different factual relations - *place in city*, *country capital city*, *person occupation*, *plays pro sport*, *company hq*, and *product by company*. For each of these examples we randomly select another example within the same relation  $(s^*, r, o^*)$  such that  $s \neq s^*$  and  $o \neq o^*$ . The average indirect effect (IE) of applying activation patching over these 400 examples is depicted on Figures 2b, 3, 5 for Mamba-2.8b) and on Figure 9 (for Pythia-2.8b).

## B Isolating The Contribution of $W_o^{(\ell)}$

Recall from Figure 1 and Equation (2) that when  $o_i^{(\ell)}$  is restored, the  $s_i^{(\ell)}$  and  $g_i^{(\ell)}$  are restored as well. To isolate the contribution of only  $W_o^{(\ell)}$  we subtract out  $\text{IE}_{s_i^{(\ell)}} + \text{IE}_{g_i^{(\ell)}}$  from  $\text{IE}_{o_i^{(\ell)}}$  and plot the results on Figure 8. Notice that, subtracting  $\text{IE}_{s_i^{(\ell)}}$  cancels out the high indirect effect at the late site shown by later layers at the last token position. But, together  $\text{IE}_{s_i^{(\ell)}} + \text{IE}_{g_i^{(\ell)}}$  cannot cancel out high  $\text{IE}_{o_i^{(\ell)}}$  of early-mid layers at the last subject token, reconfirming the mediating role of  $W_o^{(\ell)}$  in those layers while recalling a fact.

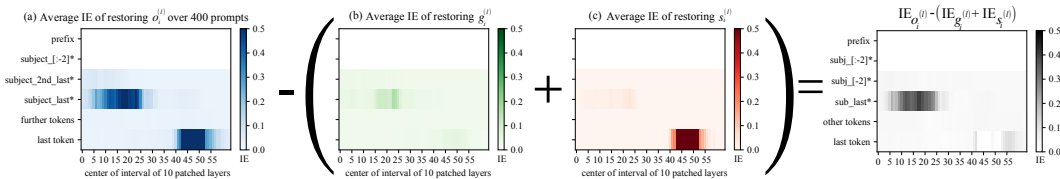


Figure 8: Isolating the contribution of  $W_o^{(\ell)}$ .  $\text{IE}_{s_i^{(\ell)}} + \text{IE}_{g_i^{(\ell)}}$  subtracted from  $\text{IE}_{o_i^{(\ell)}}$ . Notice that  $\text{IE}_{o_i^{(\ell)}} - (\text{IE}_{s_i^{(\ell)}} + \text{IE}_{g_i^{(\ell)}})$  still shows higher causal effect at the earlier site (more pronounced than  $\text{IE}_{g_i^{(\ell)}}$ ) while the high causal effect at the later site cancels out.

### C Locating Key Modules in Pythia-2.8b

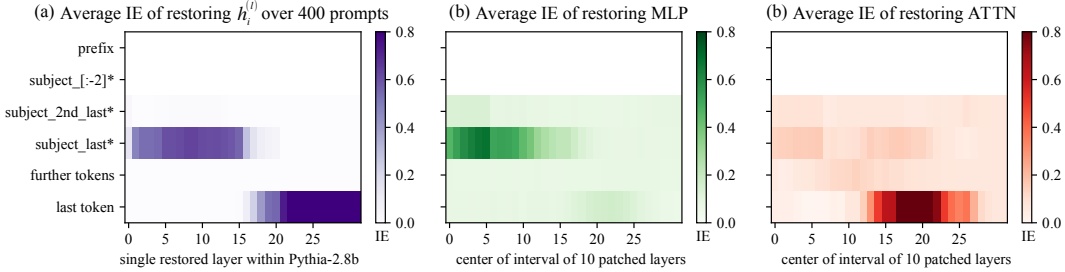


Figure 9: Average indirect effect of residual state, MLP, and attention outputs in Pythia-2.8b over 400 facts. For MLP and attention outputs a window of 10 layers around  $\ell$  is restored as restoring for just one layer barely show visible patterns.

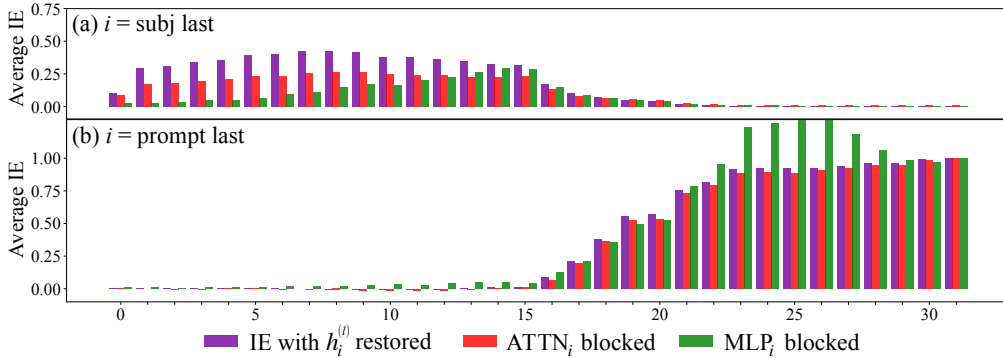


Figure 10: Impact of ablating  $\text{ATTN}_i$  or  $\text{MLP}_i$  on  $\text{IE}_{h_i^{(l)}}$  for (a) *subject last* and (b) *prompt last* token positions on Pythia-2.8b

### D Blocking Information Propagation With $s_i$ Paths

In Section 6, we discuss why surgically performing attention knock-out experiments on Mamba is challenging due to certain architectural choices - we cannot block information flow from the  $q^{\text{th}}$  token to only the  $k^{\text{th}}$  token because of the SiLU non-linearity in Equation (4). However, for a layer  $\ell$  we can block information propagation via Conv + SSM from the  $q^{\text{th}}$  token to *all* the future tokens ( $k > q$ ) by mean ablating  $a_q^{(\ell)}$ . For a window of 10 layers around  $\ell$  we block-out information propagation of the *subject*, *non-subject*, and the *prompt-last* token positions. The results plotted in Figure 11 show relative change in  $p(o)$  by blocking out  $q^{\text{th}}$  token across different layers as  $\left( p(o | a_q^{(\ell)} := \mathbb{E}[a^{(\ell)}]) - p(o) \right) / p(o)$ .

Figure 11 leads us to draw similar conclusions about information flow in Mamba as Geva et al. (2023) observe in transformer LMs.

- (a) The purple lines show that blocking out non-subject information flow in early middle layers can bring down  $p(o)$  by up to 50%. Non-subject tokens are used to specify the relation  $r$ . This observation leads us to believe that Mamba propagates relation specific information to future tokens using Conv+SSM operation in early-middle layers
- (b) Interestingly, the green lines (blocking the subject information flow) shows two valleys -
  1. The first valley at the early layers is not surprising as Mamba needs to collate information from all the subject tokens in early layers to recognize a subject entity  $s$  consisting of multiple tokens.
  2. However, the valley at layers 43 – 48 suggest that Mamba uses Conv + SSM paths in those layers to propagate critical information from the subject to later tokens. This aligns with

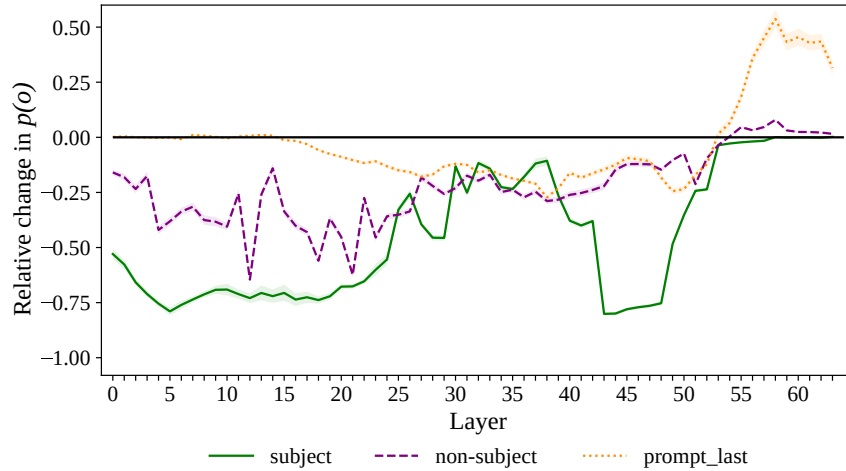


Figure 11: Relative change in  $p(o)$  when information flow to future tokens via  $s_i$  paths is blocked from either *subject*, *non-subject*, or the *prompt\_last* token positions. For each layer  $\ell$ ,  $s_i$  paths were blocked for a window of 10 layers around  $\ell$ .

Figures 5b and 3c, where  $s_i$  states in those layers show high indirect effects, indicating their crucial role while recalling a fact.

With this experiment, we cannot make strong claims on the role of the last token position (prompt-last) like Geva et al. (2023). As we block out information to *all* future tokens, the intermediate states in between the ablated token and the last token are getting corrupted as well.

## E LRE in Pythia-2.8b

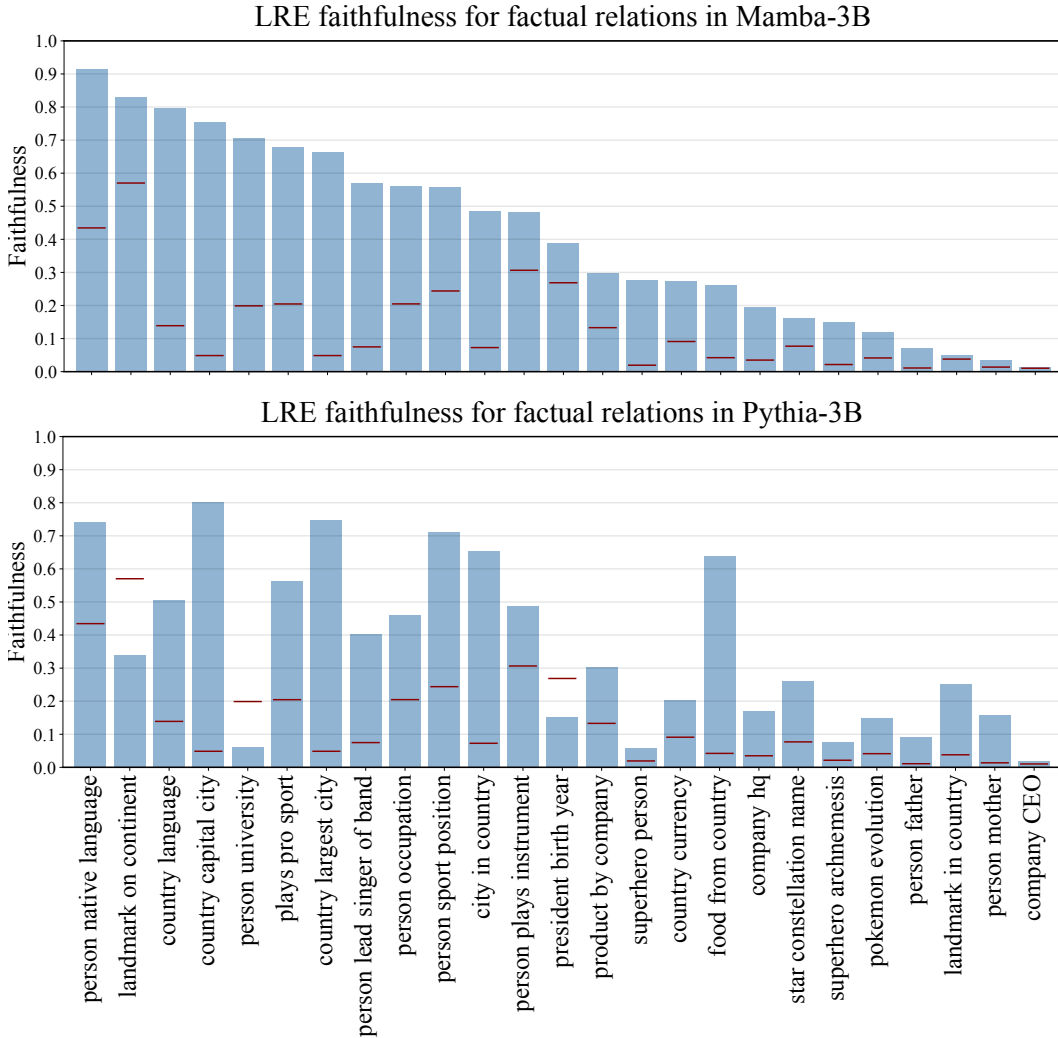


Figure 12: Relation-wise LRE *faithfulness* to the LM decoding function  $F$ . Horizontal red lines per relation indicate random-choice baseline. We only present results for the *factual* relations in the RELATIONS dataset.



## F LRE Performance Over Different Relations

Besides *faithfulness* Hernandez et al. (2023) introduced another metric *causality* to measure the performance of LRE. Since LRE is a linear function, it is invertible. Assume that for a fact  $(s, r, o)$  LRE can faithfully replace LM computation  $F(\mathbf{s}, r)$ . Then given the representation  $\mathbf{o}^*$  of another object  $o$ ,  $\mathbf{J}^{-1}(\mathbf{o}^* - \mathbf{o})$  should give us a  $\Delta\mathbf{s}$ , such that when added to  $\mathbf{s}$ ,  $\tilde{\mathbf{s}} := \mathbf{s} + \Delta\mathbf{s}$ , the model computation  $F(\tilde{\mathbf{s}}, r)$  should generate  $o^*$ . See Hernandez et al. (2023) for details on this.

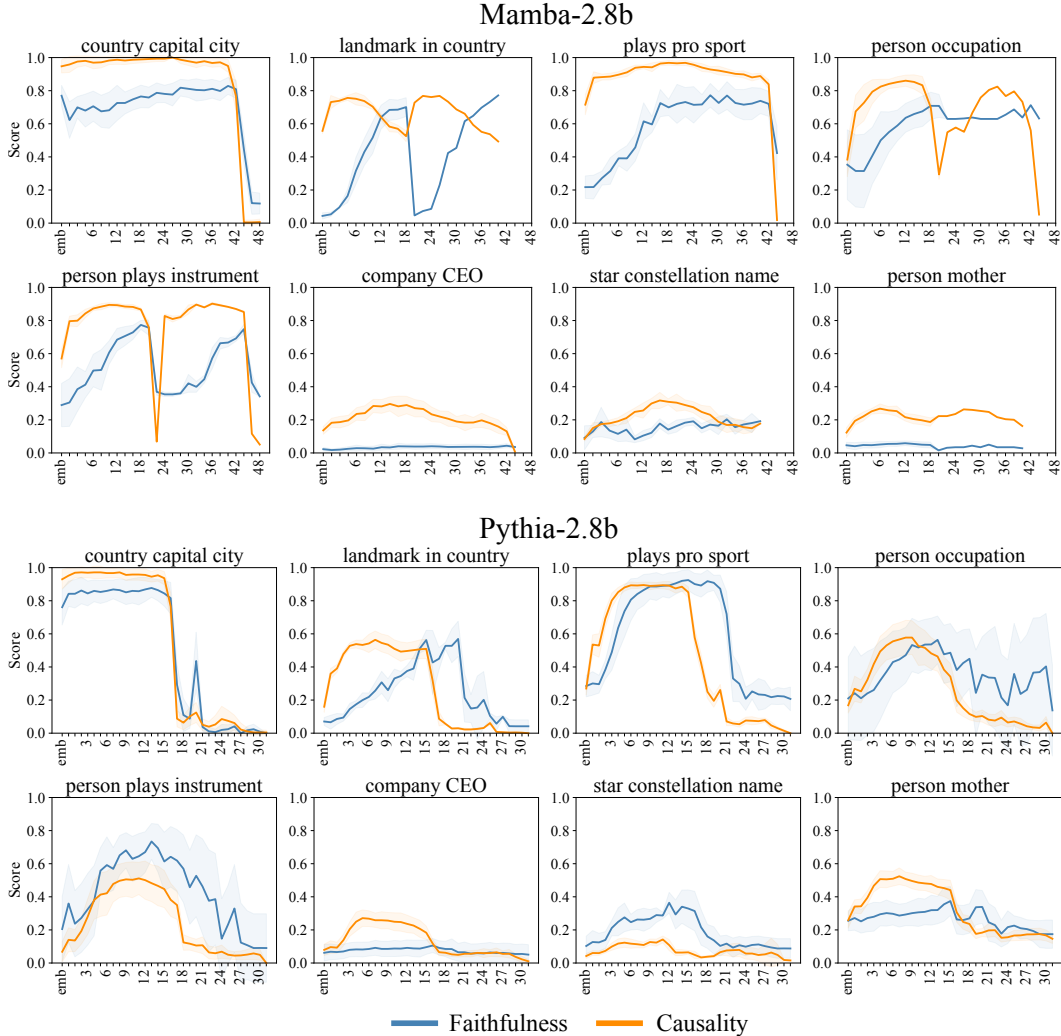


Figure 13: For Mamba, we only perform sweep till layer 48, as Figure 5 suggests negligible activity for later layers at the subject last token

## G Activation Patching Indirect Effects on Mamba-2.8b

